



MIT Open Access Articles

Randomized CRISPR-Cas Transcriptional Perturbation Screening Reveals Protective Genes against Alpha-Synuclein Toxicity

The MIT Faculty has made this article openly available. **Please share** how this access benefits you. Your story matters.

Citation	Chen, Ying-Chou et al. "Randomized CRISPR-Cas Transcriptional Perturbation Screening Reveals Protective Genes against Alpha-Synuclein Toxicity." <i>Molecular Cell</i> 68, 1 (October 2017): 247-257
As Published	http://dx.doi.org/10.1016/J.MOLCEL.2017.09.014
Publisher	Elsevier BV
Version	Author's final manuscript
Citable link	https://hdl.handle.net/1721.1/121267
Terms of Use	Creative Commons Attribution-NonCommercial-NoDerivs License
Detailed Terms	http://creativecommons.org/licenses/by-nc-nd/4.0/



Published in final edited form as:

Mol Cell. 2017 October 05; 68(1): 247–257.e5. doi:10.1016/j.molcel.2017.09.014.

Randomized CRISPR-Cas transcriptional perturbation screening reveals protective genes against alpha-synuclein toxicity

Ying-Chou Chen^{1,2,6}, Fahim Farzadfard^{1,2,3,5,6}, Nava Gharaei⁴, William C.W. Chen^{1,2}, Jicong Cao^{1,2}, and Timothy K. Lu^{1,2,3,5,7,*}

¹Synthetic Biology Group, MIT Synthetic Biology Center, Massachusetts Institute of Technology, Cambridge, MA 02139, USA.

²Research Laboratory of Electronics, Massachusetts Institute of Technology, Cambridge, MA 02139, USA.

³MIT Microbiology Program, Massachusetts Institute of Technology, Cambridge, MA 02139, USA.

⁴MCO Graduate Program, Department of Molecular and Cellular Biology, Harvard University, Cambridge, United States 02138, USA.

⁵Department of Biological Engineering and Electrical Engineering & Computer Science, Massachusetts Institute of Technology, Cambridge, MA 02139, USA.

SUMMARY

The genome-wide perturbation of transcriptional networks with CRISPR-Cas technology has primarily involved systematic and targeted gene modulation. Here, we developed PRISM (Perturbing Regulatory Interactions by Synthetic Modulators), a screening platform that uses randomized CRISPR-Cas transcription factors (crisprTFs) to globally perturb transcriptional networks. By applying PRISM to a yeast model of Parkinson's disease (PD), we identified guide RNAs (gRNAs) that modulate transcriptional networks and protect cells from alpha-synuclein (α Syn) toxicity. One gRNA identified in this screen outperformed the most protective suppressors of α Syn toxicity reported previously, highlighting PRISM's ability to identify modulators of important phenotypes. Gene expression profiling revealed genes differentially modulated by this strong protective gRNA that rescued yeast from α Syn toxicity when overexpressed. Human homologs of top-ranked hits protected against α Syn-induced cell death in a human neuronal PD model. Thus, high-throughput and unbiased perturbation of transcriptional networks via randomized crisprTFs can reveal complex biological phenotypes and effective disease modulators.

Graphical abstract

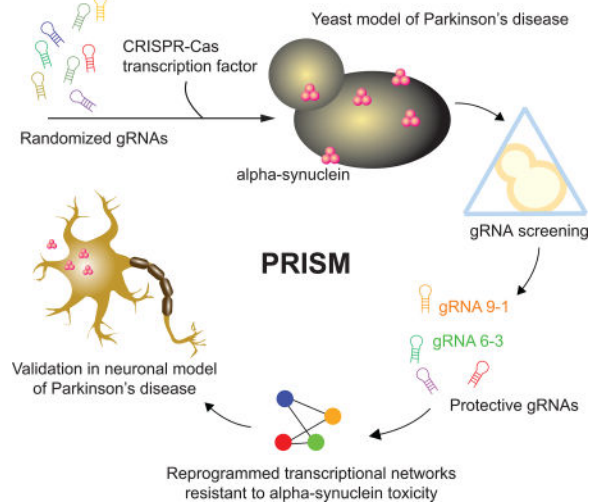
*Correspondence: timlu@mit.edu.

⁶These authors contributed equally

⁷Lead Contact

AUTHOR CONTRIBUTIONS

YCC, FF and TKL designed experiments, analyzed data, discussed results and wrote the manuscript. YCC and FF performed yeast experiments. FF and NG designed RNA-Seq experiments and analyzed data. YCC performed mammalian cell experiments. WC and JC helped with mammalian cell experiments.



INTRODUCTION

The systematic perturbation of transcriptional networks enables the elucidation of gene functions and regulatory networks that underlie biological processes. Current methods of modulating transcriptional networks mainly rely on targeted single-gene overexpression, knockout, and knockdown (Boutros and Ahringer, 2008; Carpenter and Sabatini, 2004; Costanzo et al., 2016; Forsburg, 2001). With the advent of artificial transcription factors, such as zinc-finger-, Transcriptional Activator-Like Effector (TALE)-, and CRISPR-Cas9-based transcription factors (crisprTFs), customized transcriptional perturbations are possible (Blancafort et al., 2005; Carroll, 2014; Park et al., 2003; Zhang et al., 2011). For example, crisprTF-based platforms enable bi-directional gene activation and repression in eukaryotic systems (Chavez et al., 2015; Farzadfard et al., 2013; Gilbert et al., 2013; Mali et al., 2013; Nishimasu et al., 2014; Zalatan et al., 2015) and have been used for genome-wide targeted screens owing to the ease of designing and synthesizing guide RNAs (gRNAs) (Gilbert et al., 2014; Horlbeck et al., 2016; Konermann et al., 2015). In addition, strategies for higher-order perturbations using barcoded combinatorial genetic screens in human cells have been adapted to be compatible with CRISPR-Cas9 screens (Wong et al., 2015; Wong et al., 2016). Existing CRISPR-Cas9-based screening strategies rely on gRNAs designed to target individual genes while minimizing off-target effects (Cencic et al., 2014; Frock et al., 2015; Gilbert et al., 2014; O'Geen et al., 2015; Parnas et al., 2015; Shalem et al., 2014; Wang et al., 2014; Wu et al., 2014). Although these technologies provide powerful strategies for perturbing individual genes, they may not be suitable for global or combinatorial perturbation of transcriptional networks. Many complex diseases, as well as treatments required to counteract those conditions, may involve simultaneous or dynamic changes in the expression levels of many genes, which are not accessible by screens that target genes one at a time (Khurana et al., 2017; Yeger-Lotem et al., 2009).

To address this limitation, we explored the use of randomized gRNAs and crisprTFs in an approach called PRISM (Perturbing Regulatory Interactions by Synthetic Modulators) in order to effect global transcriptional perturbations conferring enhanced cellular resistance to

alpha-synuclein (α Syn). The aggregation of misfolded α Syn in intraneuronal Lewy bodies is one of the pathological hallmarks of Parkinson's disease (PD) (Goedert et al., 2013; Spillantini et al., 1997). The overexpression of α Syn in various eukaryotic model organisms has been used to elucidate the complex cellular processes associated with PD (Lashuel et al., 2013; Maries et al., 2003; Wong and Krainc, 2017). Because of its conserved molecular mechanisms and the availability of genetic tools, *Saccharomyces cerevisiae* has been extensively used as a model to systematically study and identify genes involved in neurodegenerative diseases such as PD and Alzheimer's disease (Khurana and Lindquist, 2010; Tardiff et al., 2014).

Here, we demonstrate that one of the strongest protective gRNAs identified in our PRISM screens outperformed any individual overexpressed gene that we tested in suppressing α Syn toxicity, including the strongest protective genes found in previous genome-wide screens (Cooper et al., 2006; Gitler et al., 2009; Tenreiro et al., 2016; Yeger-Lotem et al., 2009). These results highlight that randomized gRNA/crisprTF perturbations can achieve powerful phenotypic modulation compared with other targeted gene perturbation methods.

RANDOMIZED gRNA SCREENING DESIGN

We cloned a dCas9-VP64 expression cassette under the control of a doxycycline (Dox)-inducible (Tet-ON) promoter. To build the yeast screen strain, this construct was integrated into the genome of an α Syn-expressing *S. cerevisiae* strain (hereafter referred to as the yeast parental strain) in which two copies of the human wild-type α Syn (*SNCA*) gene fused to yellow fluorescent protein (YFP) are overexpressed under the control of a galactose (Gal)-inducible promoter (Cooper et al., 2006) (Figure 1A). Both the yeast parental strain and the screen strains showed significant cellular growth defects in the presence of Gal due to overexpression of α Syn. The expression of dCas9-VP64 with no gRNA in the screen strain did not interfere with normal cellular growth or α Syn-associated toxicity (Figure S1A).

A randomized gRNA-expressing plasmid library was built by co-transforming the screen strain with linearized high-copy 2μ plasmids, flanked by the *RPR1* promoter (*RPR1p*) and gRNA handle at the ends, and a randomized oligo library encoding 20-mer randomized nucleotides flanked by homology arms to the ends of the vector (Figure 1A). We observed approximately 100 million colony forming units (CFUs) per library transformation, which is comparable with the theoretical diversity of the seed sequence, the protospacer adjacent motif (PAM)-proximal 12 nucleotides ($4^{12} = \sim 1.67 \times 10^7$). Library representation and sequence distributions were determined by deep sequencing (Figures S2A–S2G). After cells were transformed with the library, they were recovered in liquid culture with Dox (1 μ g/mL) for 12 hours to amplify the library and induce crisprTF expression. The cultures were then plated on synthetic complete media (Scm)–Uracil (Ura)+Gal+Dox plates, and gRNAs from surviving colonies were characterized by colony PCR followed by Sanger sequencing.

RESULTS

gRNA Suppressors of α Syn Toxicity were Identified by a Randomized Screen in *Saccharomyces cerevisiae*

To validate the activity of the identified gRNAs, they were re-cloned in both high-copy 2μ and low-copy *ARS/CEN* plasmids, and transformed back into both parental and screen strains. We confirmed that two gRNAs (designated as gRNA 6-3 and gRNA 9-1), expressed from either high-copy and low-copy plasmids, could rescue the screen strain from α Syn toxicity (Figure 1B). gRNA 6-3 moderately suppressed α Syn toxicity whereas gRNA 9-1 strongly suppressed it; gRNA 9-1 was thus chosen for further characterization. Although no perfect match between the identified gRNAs and the yeast genome was found, relaxing the search criteria (to find up to two mismatches inside the seed region) revealed the presence of a few dozen sites that could potentially serve as off-target binding sites of these gRNAs, including one in the *GAL4* gene (Table S1). As additional controls, we confirmed that gRNA 9-1-mediated suppression of α Syn toxicity relied on the presence of dCas9-VP64 (Figure S1B) and that *GAL4* and α Syn expression levels were not directly affected by gRNA 9-1/crisprTF (Figures S1E–S1F). Furthermore, we re-encoded the putative gRNA 9-1 off-target binding site in *GAL4* so that there were five matches in the seed sequence and found that gRNA 9-1 preserved its ability to rescue the screen yeast strain from α Syn toxicity (Figures S1G–S1I).

Gene Expression Profiling of α Syn-resistant Cells by gRNA 9-1/crisprTF Revealed Suppressors of α Syn Toxicity

We compared the transcriptome of screen cells expressing gRNA 9-1 and dCas9-VP64 to that of cells expressing dCas9-VP64 but no gRNA by using RNA sequencing to map transcriptional perturbations enacted by the α Syn-protective crisprTF (Figure 1C and Figures S2H–S2I). We identified 114 differentially expressed genes with at least two-fold changes in mRNA expression levels compared with the non-gRNA control (false discovery rate (FDR)-adjusted p-value = 0.1) (Table 1 and Table S2). Most of these genes (93%) have not been previously identified in single gene knockout or overexpression screens as suppressors of α Syn toxicity (Cooper et al., 2006; Gitler et al., 2009; Yeger-Lotem et al., 2009). Intriguingly, they were enriched in Gene Ontology (GO) categories including protein quality control, ER/Golgi trafficking, lipid metabolism, mitochondrial function, and stress responses (Table S3). Almost all of the newly identified genes exhibited only modest changes in gene expression (109 out of 114 genes had fold-changes <5).

We systematically tested the effects of our differentially expressed genes on α Syn toxicity in the screen strain by overexpressing 95 of them that were found in the Yeast ORF Collection (Open Biosystems). Overexpression of 57 out of 95 (60%) genes (13 down-regulated and 44 up-regulated by gRNA 9-1/crisprTF) significantly suppressed α Syn toxicity (Figure S3A, summarized in Table S2; representative candidates are shown in Figure 2A), whereas only 5 out of 34 (14.7%) genes randomly chosen from the Yeast ORF Collection suppressed α Syn toxicity (Figure S3B and Table S4). Thus, our randomized gRNA/crisprTF screening approach enriched the search for α Syn-toxicity suppressors.

Furthermore, there was no significant correlation between observed α Syn expression levels and toxicity (Figures S1E–S1F). *UBP3* (ubiquitin-specific protease) was used as a positive control. *UBP3*, previously shown to be a strong suppressor of α Syn toxicity, is known to participate in the degradation of misfolded proteins in the vesicular trafficking processes (Chung et al., 2013; Cooper et al., 2006; Tardiff et al., 2013). We found that 29 genes whose expression was modulated by gRNA 9-1 protected against α Syn-toxicity similarly to or better than *UBP3*. Notably, gRNA 9-1 alone outperformed the overexpression of any single gene in abrogating α Syn-associated phenotypes based on cell viability assay results, shown in Figure 2A and microscopy (see below and Figures S4A–S4B), suggesting that gRNA 9-1 plays a master role in mitigating α Syn stress.

Alterations in membrane trafficking and localization of α Syn from the plasma membrane into cytoplasmic foci are well-established hallmarks of PD (Outeiro and Lindquist, 2003). Owing to highly conserved mechanisms involved in membrane trafficking, yeast cells have been used to study α Syn-coupled vesicular trafficking defects, which has led to mechanistic insights into modifiers of α Syn toxicity, such as *UBP3* and the Rab family GTPase *YPT1* and their human homologs (Chung et al., 2013; Cooper et al., 2006; Tardiff et al., 2013). We quantitatively measured the effect of gRNA 9-1 on the localization of α Syn-YFP by microscopy. In this assay, aggregated α Syn-YFP is detected as cytoplasmic foci, which are distinguishable from the membrane-localized, non-aggregated form of the protein. As shown in Figures 2B and 2C, upon 6 hours of α Syn induction, 92% of yeast cells with dCas9-VP64 but no gRNA (negative control) contained aggregated α Syn-YFP foci. Overexpression of dCas9-VP64 along with gRNA 9-1 resulted in localization of α Syn-YFP to the plasma membrane such that aggregated α Syn-YFP foci were observed in only ~7% of cells. This was significantly lower than the percentage of cells overexpressing *UBP3* (~39% cells with α Syn-YFP foci), which we used as a positive control.

Human *DJ-1/PARK7*, *ALS2*, *GGA1*, and *DNAJB1* Homologs were Identified as Robust Protectors against α Syn Toxicity

One of the interesting functional categories identified in our screen involves the heat shock chaperones. Specifically, *HSP31–34* heat shock proteins are homologs of the human *DJ-1/PARK7* gene, in which autosomal recessive mutations are associated with early onset of familial PD (Bonifati et al., 2003). *DJ-1* is thought to protect neurons from mitochondrial oxidative stress by acting as a redox-dependent chaperone to inhibit α Syn aggregates (Bonifati et al., 2003; Canet-Aviles et al., 2004). The roles of *HSP31–34* in protecting yeast cells from α Syn toxicity have been previously investigated (Zondler et al., 2014); however, these genes have not been identified in previous genome-wide screens for modifiers of α Syn toxicity. We identified *SNO4/HSP34* and *HSP32* as two of the differentially expressed genes in our screen. As shown in Figure 2, either *SNO4/HSP34* or *HSP32*, when overexpressed, significantly rescued α Syn-induced growth defects and membrane-trafficking abnormalities. Interestingly, *SNO4/HSP34* was moderately up-regulated by gRNA 9-1, whereas *HSP32* was extremely down-regulated (Figure 1C and Table 1), which could reflect evolutionarily conserved functions of these paralog proteins, despite their being under the control of different gene regulatory programs. Furthermore, overexpression either of the other two yeast *DJ-1* homologs (*HSP31* and *HSP33*) also significantly suppressed α Syn toxicity

(Figure 2A), even though they were not significantly modulated by gRNA 9-1. This further supports the involvement of this class of paralog heat-shock proteins in suppressing α Syn toxicity. Consistently, *HSP31* (which among *HSP31–34* shows the least homology with *DJ-1*) was recently shown to be a chaperone involved in mitigating various protein misfolding stresses, including that of α Syn (Tsai et al., 2015).

Among other top α Syn-toxicity suppressors (Table 1 and Figure 2), yeast *SAF1* encodes an F-Box protein that selectively targets unprocessed vacuolar/lysosomal proteins for proteasome-dependent degradation (Escusa et al., 2007; Mark et al., 2014). The homolog of this protein in mice and humans, *ALS2/alsin*, functions as a guanine nucleotide exchange factor (GEF) that activates the small GTPase *Rab5*, an evolutionarily conserved protein involved in membrane trafficking in endocytic pathways (Hadano et al., 2007). Mutations in human *ALS2* have been shown to cause autosomal recessive motor neuron diseases (Chandran et al., 2007). In addition, we found that *GGA1* and its paralog *GGA2* could both alleviate α Syn toxicity (Figures 2 and S3), which was interesting because neither of them had been reported previously to have this activity. The yeast *GGA1* protein has been implicated in binding ubiquitin, thus facilitating the sorting of cargo proteins from the trans-Golgi network to endosomal compartments (Takatsu et al., 2002; Zhdankina et al., 2001). Human *GGA1* overexpression attenuates amyloidogenic processing of amyloid precursor proteins (APP) in Alzheimer's disease and a rare inherited lipid-storage disease, Niemann-Pick type C (NPC) (Kosicek et al., 2014; von Einem et al., 2015). Finally, *SIS1*, the yeast Hsp40 homolog of human *DNAJ/HSP40* family proteins, was identified as α Syn suppressor via PRISM. *DNAJ* family proteins play roles in priming the specificity of *HSP70* chaperoning complexes. It has been shown that mammalian *DNAJ* and *HSP70* are up-regulated in response to α Syn overexpression (Vos et al., 2008). In addition, the *DNAJB* subfamily has been shown to suppress polyglutamine (polyQ) aggregates (Gillis et al., 2013). These results demonstrate that randomized transcriptional perturbations with PRISM enable the discovery of modulators of disease-relevant phenotypes.

Verification of Human Homologs of the Identified Hits in a Neuronal PD Model

To investigate the neuroprotective effects of the human homologs of the protective yeast genes described above, we overexpressed *DJ-1*, *ALS2*, *GGA1*, and *DNAJB1* in an α Syn-overexpressing human neuroblastoma cell line (SH-SY5Y), an established neuronal model of PD (Vekrellis et al., 2009). SH-SY5Y cells were differentiated into cells with dopaminergic neuron-like phenotypes upon retinoic acid (RA) treatment. When β -galactosidase (β -gal) was expressed in these cells, no toxicity was observed. In contrast, α Syn-expressing cells gradually exhibited neurite retraction and only 40–50% viability at 6 days of differentiation (Figures S5A–S5B). Expressing *DJ-1* or *ALS2* alone did not alter cell survival in the absence of α Syn, but strongly suppressed α Syn-inducible cell death (Figure 3B). α Syn-expressing cells that were transfected with *GGA1* or *DNAJB1* exhibited about 60% viability, which was similar to the effect of expressing the known anti-apoptotic gene *Bcl-xL* (positive control). Consistent with these results, overexpression of *DJ-1* or *ALS2* resulted in reductions in the dead cell populations, as did treatment with the apoptotic inhibitor zVAD (Figure 3C).

Human *TXN* and *TIMM9* Synergistically Protect Cells against α Syn Toxicity

Increased oxidative stresses and defective mitochondrial function are pathological mechanisms involved in sporadic PD (Henchcliffe and Beal, 2008). We identified that yeast thioredoxin *TRX1*, an oxidoreductase involved in maintaining the cellular redox potential, and *TIM9*, a mitochondrial chaperone involved in the transport of hydrophobic proteins across mitochondrial intermembrane space (Neupert and Herrmann, 2007), participate in the suppression of α Syn toxicity in yeast cells (Figure 2 and Figures S4C–S4E). Neuronal cells transfected with the human homologs of either of these genes, *TXN* or *TIMM9*, respectively, exhibited about ~60% survival upon α Syn induction compared with <50% with the vector control expressing no transgene. Intriguingly, co-expression of the two human genes *TXN* and *TIMM9* led to enhanced survival in the presence of α Syn toxicity (~88 % survival) (Figure 3D). Furthermore, the neuroprotective effects of expressing *DJ-1*, *TXN*, and *TIMM9* were specific to α Syn-associated toxicity, as these genes did not protect against 1-methyl-4-phenyl pyridinium (MPP⁺)-induced neurodegeneration (Dietz et al., 2008) (Figure 3E and Figures S5C–S5D).

To further investigate these genes as potential therapeutic targets for neuroprotection in PD, we engineered lentiviral vectors expressing *DJ-1*, *TXN*, or *TIMM9*, or co-expressing *TXN* and *TIMM9*. We then used these vectors to stably infect cells prior to inducing α Syn stress. Consistent with our transient transfection experiments, *DJ-1* reliably protected differentiated SH-SY5Y cells from α Syn-induced cell death and neuronal abnormalities, as did co-expression of *TXN* and *TIMM9* (Figure 4). These results also suggest that activation of these endogenous genes could be explored as a potential therapeutic direction for neuroprotection in PD.

DISCUSSION

In this study, we introduce the PRISM screening platform to probe mechanisms underlying cellular responses to α Syn stress. This platform takes advantage of the promiscuity of crisprTF activity with randomized gRNAs for global transcriptional network perturbations. In contrast to typical targeted CRISPR screens, in which gRNAs are designed to modulate individual genes, PRISM does not require any assumptions regarding potential targets and enables unbiased and high-level perturbations of cellular networks. Thus, randomized gRNA screening with PRISM is complementary to targeted screening strategies that have been used with CRISPR-Cas nucleases, crisprTFs, and RNA interference (Blancafort et al., 2005; Demir and Boutros, 2012; Gilbert et al., 2014; Konermann et al., 2015; Moffat et al., 2006; Park et al., 2003; Parnas et al., 2015; Paulsen et al., 2009; Root et al., 2006; Santos and Stephanopoulos, 2008; Shalem et al., 2014; Wang et al., 2014; Whitehurst et al., 2007; Wong et al., 2015; Wong et al., 2016). Randomized gRNA screening with crisprTFs involves a simple library construction procedure and enables global perturbations of transcriptional networks that might not be accessible by traditional single- or multiple-gene perturbations. Such high-order perturbations may be especially important when studying sophisticated phenotypes involving multi-layered regulatory networks, such as those associated with complex human diseases or stress tolerance.

As a proof of concept, we applied this system to a yeast model of PD and identified a diverse set of differentially expressed genes that could individually and collectively rescue α Syn-associated phenotypes. Transcriptomic analysis of the top α Syn-toxicity-protecting gRNA candidate (gRNA 9-1) revealed modest changes in the expression of multiple genes involved in various pathways associated with PD. Intriguingly, genes perturbed by gRNA 9-1 were enriched for α Syn toxicity suppressors versus random selection, most of which have not been reported in previous unbiased genome-wide screens. We verified that over half of these newly identified genes, when overexpressed, rescued yeast cells from α Syn-mediated toxicity. Moreover, gRNA 9-1/crisprTF ameliorated α Syn-associated phenotypes more than overexpression of any individual gene, highlighting the power of global transcription factor screening and suggesting that combinatorial or global effects can enhance desired phenotypes.

To verify the physiological relevance of our hits, we overexpressed the human homologs of validated yeast hits in a human neuronal model of α Syn toxicity. Interestingly, human genes *TXN* and *TIMM9*, homologous to yeast genes *TRX1* and *TIM9*, respectively, worked synergistically to suppress α Syn toxicity in human cells (Figure 4). Thioredoxin is known to facilitate the mitochondrial import of *TIM9* in yeast (Durigon et al., 2012) and to act as a neuroprotective agent against oxidative stress in neuronal cells (Lin and Beal, 2006). The observed synergistic effect of *TXN* and *TIMM9*, as well as the protective effect of redox-dependent chaperones, in suppressing α Syn toxicity further points to the potential importance of mitochondrial maintenance and oxidative stress in PD. Future efforts will be needed to determine whether combinatorial modulation of mitochondrial function pathways and cellular redox may help treat α Syn-associated dysfunction in animal models and clinical settings. In addition, future work should investigate the underlying mechanisms of neuroprotection from the hits identified in this study. These insights could help to develop neuroprotective strategies or engineer α Syn-resistant neuronal cells that could help prevent progressive neurodegeneration in PD patients diagnosed early.

LIMITATIONS

In this screening effort, we used a first-generation crisprTF that results in modest levels of gene activation or repression (Farzadfard et al., 2013; Gilbert et al., 2014). Stronger activation and repression could be achieved by recently improved variants of crisprTFs (Chavez et al., 2015; Konermann et al., 2015; Tanenbaum et al., 2014) while other types of perturbations could be introduced via dCas9 fused to epigenetic regulatory domains (Hilton et al., 2015; Kearns et al., 2015; Thakore et al., 2015).

We performed Sanger sequencing on the surviving colonies to identify gRNA 9-1 and gRNA 6-3, which were then tested in validation experiments. In several cases, we identified multiple different gRNAs within a single yeast cell. Performing high-throughput sequencing on amplicons obtained from surviving yeast colonies could reveal additional gRNAs that could rescue cells from α Syn toxicity when combinatorially expressed. However, for the purpose of this study, we chose to focus only on individual gRNAs that had suppressive effects against α Syn toxicity on their own. In future work, yeast single-copy centromeric

(*ARS/CEN*) plasmids could be used for gRNA expression to ensure that each transformant receives only one gRNA variant.

Even though many genes were up- or down-regulated by gRNA 9-1, we validated them only through overexpression using the readily available Yeast ORF Collection. Thus, our current data suggests that genes modulated by gRNA hits from PRISM screens are enriched for effects on the desired phenotype, but does not indicate the impact of directionality of gene modulation on the phenotype. In future work, genes identified via PRISM screens can be tested via knockdown as well as overexpression in order to determine whether directionality makes a difference. Furthermore, we chose to overexpress genes from the *GALI* promoter in the Yeast ORF Collection rather than using CRISPR activation because efficient targeted CRISPR activation still requires tuning and optimization for each gene of interest. However, overexpression of ORFs by the strong *GALI* promoter can result in expression levels much higher than those achievable by our first-generation crisprTFs. In future work, assessing how different expression levels of identified genes modulate the phenotypes identified through PRISM screening will also be of interest. Finally, we envision that genetic interactions between genes identified by PRISM screening can be further mapped through combinatorial CRISPR technologies (Han et al., 2017; Shen et al., 2017; Wong et al., 2016) and both gene activation and inhibition technologies. Thus, high-throughput randomized crisprTF screens should provide access to a broader range of biological phenotypes across a wide range of organisms in the future.

We predicted 51 potential binding sites for gRNA 9-1 in the yeast genome (Table S1). Although direct crisprTF binding should be identifiable by Chromatin Immunoprecipitation Sequencing (ChIP-Seq) experiments, we were unable to achieve this despite trying multiple different approaches (Kuscu et al., 2014; O'Geen et al., 2015; Wu et al., 2014). We hypothesize that this may be due to weak binding of dCas9 in the absence of perfect-match binding sites for gRNA 9-1 in the genome. Furthermore, it remains challenging to infer transcription regulatory networks solely based on predicted crisprTF binding sites and changes in RNA levels without mapping the transient and indirect cascades involved in transcriptional perturbations (MacQuarrie et al., 2011). Therefore, drawing direct connections between crisprTFs and regulated genes in PRISM screens remains a challenge that needs to be addressed in future work.

STAR METHODS

Contact for Reagent and Resource Sharing

Further information and requests for resources and reagents should be directed to and will be fulfilled by the Lead Contact, Timothy K. Lu (timlu@mit.edu).

Experimental Model and Subject Details

Yeast Strains and Growth Condition—Strains used in this study are all derivatives of W303 (MATa *ade2-1 trp1-1 can1-100 leu2-3, 112 his3-11, 15 ura3*). The ITox2C yeast strain (Cooper et al., 2006) harboring two copies of wild-type α Syn (*SNCA*)-YFP under control of the Gal-inducible *GALI* promoter (hereafter referred to as the parental strain, a

generous gift from Dr. Susan Lindquist, Whitehead Institute, USA) was used for the construction of the crisprTF-expressing screen strain. The Dox-inducible (Tet-ON) promoter was constructed by cloning the pTRE promoter and reverse tetracycline-controlled transactivator (rtTA, from Addgene plasmid #31797) upstream of a minimal *CYCI* promoter in the pRS405 backbone. The dCas9-VP64 expression cassette (Addgene plasmid #49013) was then cloned into this vector using Gibson assembly. A sense mutation was introduced within the *LEU2* ORF by using the QuikChange system (Stratagene) in order to generate a unique PstI site in the vector. The pRS405-pTetON-dCas9-VP64-PstI plasmid was linearized by PstI and transformed into ITox2C parental strain to build the screen strain. Leucine-positive integrants were verified by genomic PCRs as well as testing for the presence of α Syn-mediated defects by the survival assay and microscopy after Gal induction.

To build the *GAL4** strain, a sequence containing full endogenous *GAL4* promoter (−257 to 214) was first PCR amplified by oligos (forward: 5'-CCCAGTATTTTTTTTATTCTACAAACC -3'; reversed: 5'-AAATCAGTAGAAATAGCTGTTCCAGTCTTTCTAGCCTTGATTCCACTTCTGTCAGgT GaGcTcgGttaaCGGAGACCTTTTGGTTTTGG -3'). This fragment was then assembled (by Gibson assembly) with a kanMX6 expression cassette amplified from pFA6a-kanMX (Addgene plasmid #39296) using oligos (forward: 5'-GGGGCGATTGGTTTGGGTGCGTGAGCGGCAAGAAGTTTCAAACCGTCCGCGTCC TTTGAGACAGCATTCGGAATTCGAGCTCGTTTAAAC -3'; reversed: 5'-GAAGTTTTGTAGAATAAAAAAATACTGGGCGGATCCCCGGGTAAATTA -3'). The assembled kanMX-*GAL4** cassette was then purified and transformed into yeast cells and transformants were selected in presence of 200 mg/L G418 (Thermo Fisher Scientific). Integrants were confirmed by yeast colony PCR and Sanger sequencing.

Yeast cells were cultured in either YPD (1% yeast extract, 2% Bacto-peptone and 2% glucose) or Synthetic complete medium (Scm) supplemented with 2% glucose, raffinose, or galactose. Doxycycline (Sigma) was added directly to culture media or plates immediately before pouring (final concentration of 1 μ g/mL).

Neuroblastoma Cell Culture and Gene Expression—Parental and engineered SH-SY5Y cell lines (Vekrellis et al., 2009) (kindly provided by Dr. Leonidas Stefanis, Biomedical Research Foundation Academy Of Athens, Greece) were grown in Dulbecco's Modified Eagle Medium/Nutrient Mixture F-12 (DMEM/F-12) base medium plus 1% GlutaMAX™ supplemented with 15% heat-inactivated FBS (Fetal Bovine Serum) and 1 \times antibiotic-antimycotic (Invitrogen) at 37 °C with 5% CO₂. Cells were seeded at an initial density of 10⁴ cells/cm² in culture dishes coated with 0.05 mg/mL collagen (Invitrogen). Cells were maintained with 2 μ g/mL Dox as previously described (Vekrellis et al., 2009), in order to repress expression of α Syn and β -galactosidase (β -gal), which are driven by the Tet-OFF promoter (Gouarne et al., 2015; Vekrellis et al., 2009). The expression of α Syn and β -gal was induced by removing Dox from the media. Cells were differentiated by treating the cells with 10 μ M all-trans Retinal (RA; Sigma) for 6 days. For transient expression of human genes, cells were transfected by adding 1 μ g plasmid DNA/ 4 μ L FuGENE® HD Transfection Reagent (Promega).

Lentivirus production and transduction were performed as previously described (Lois et al., 2002). Viral supernatants from HEK-293T fibroblasts were collected at 48-hr after transfection, and filtered through a 0.45 μ m polyethersulfone membrane. For transduction with individual vector constructs, 2 ml filtered viral supernatant was used to infect 2×10^6 cells in the presence of 8 μ g/mL polybrene (Sigma) overnight. Cells were washed with fresh culture medium 1 day after infection, and cultured for following 6 days before RA treatment and α Syn induction.

Method Details

Randomized gRNA Library construction and Screening—To build the randomized gRNA library, random oligos containing 20 bp random nucleotide flanked by homology arms to the vector were co-transformed into yeast with a linearized 2 μ vector flanked by *RPR1* promoter and gRNA handle at the ends into the screen yeast strain. Once inside the cells, a gRNA-expressing library was reconstituted by the yeast homologous recombination machinery. The randomized oligo library was synthesized by the IDT hand-mixed protocol for randomized oligos using the following template: 5'-GCTGGGAACGAAACTCTGGGAGCTGCGATTGGCAG(N1:32181832)(N1)GTTTTAGAGCTAGAAATAGCAAGTTAAATAAGGC-3', where N1 indicates the hand-mixed nucleotide with the following ratio: A:C:G:T = 32:18:18:32. The GC content of the randomized portion of the oligo pool was set to 64% to match with the average GC content of yeast promoters (<http://rulai.cshl.edu/SCPD/>). The libraries were screened in the presence of both galactose and Dox, and the gRNA content of surviving colonies were characterized by colony PCR followed by Sanger sequencing. Individual gRNAs were verified by cloning each gRNA sequence into the empty gRNA vector and transforming these vectors back into the screen strain to validate gRNA activity in a clean background.

Yeast Growth and Viability Assays—The yeast screen strain was transformed with gRNAs or individual genes obtained from yeast ORF library (Open Biosystems). Single transformant colonies were grown overnight in Scm-Uracil (Ura)+raffinose media in the presence of Dox (1 μ g/mL) to induce crisprTF expression. Saturated cultures were diluted to OD₆₀₀ = 0.1 in Scm-Ura+Glucose+Dox and Scm-Ura+Galactose+Dox media and grown at 30 °C in a Synergy H1 Microplate Reader (BioTek). OD₆₀₀ and fluorescence (excitation and emission spectrum at 508 and 534 nm, respectively) were monitored over the course of the experiments. For measuring cell viability by spotting assays (Chen et al., 2013), cultures were serially diluted (5-fold dilutions) and spotted on Scm-Ura+Glucose+Dox plates for visualizing total viable cells and on Scm-Ura+Galactose+Dox plates for measuring survival. Plates were incubated at 30 °C for 2 days.

RNA Preparation and Sequencing—The screen strain was transformed with either a vector expressing gRNA 9-1 or the empty gRNA vector. Two single-colony transformants from each sample were grown overnight in Scm-Ura+Glucose+Dox. These cultures were diluted into the same fresh media to OD₆₀₀ = 0.1 and were incubated at 30 °C, 300 RPM. Samples were collected in mid-logarithmic phase (OD₆₀₀ = 0.8) and flash-frozen in liquid nitrogen. Samples were kept in -80 °C until further processing. Total RNA samples were

prepared using the MasterPure Yeast RNA Purification kit (Epicentre) following the manufacturer's protocol. mRNA libraries were prepared using the Illumina TruSeq library preparation kit, barcoded, multiplexed and sequenced by Illumina HiSeq. The reads were processed by the MIT BioMicroCenter facility pipeline and mapped to the *S. cerevisiae* reference genome (sacCer3). RPKM values were calculated using ArrayStar and differentially expressed genes were identified by t-test (p-value ≤ 0.1 , FDR correction (Benjamini, 1995)). Genes that exhibited at least twofold changes in expression in cells containing the gRNA 9-1 compared with the reference (empty gRNA vector) were considered as differentially expressed. Functional classification of the identified genes was performed using the FunSpec webserver (Robinson et al., 2002).

Western Blotting and Fluorescence Imaging—Yeast protein extracts were prepared for Western blotting by trichloroacetic acid extraction (Chen and Weinreich, 2010). Blots were probed in phosphate-buffered saline containing 0.1% Tween containing 1% (w/v) dried milk. Overexpression constructs containing a 6×His tag were detected using anti-His monoclonal antibody (1:2000; R93025, Life Technologies) followed by anti-mouse-HRP secondary antibody. α Syn (*SNCA*) was detected with mouse monoclonal anti- α Syn antibodies (1:1000; Syn-1/Clone 42, BD Biosciences).

α Syn-YFP expressing cells were directly visualized under an inverted fluorescence microscope (Zeiss) after 6 days of α Syn induction. The phenotypes were quantified by counting α Syn foci in at least 100 individual cells in multiple randomly chosen fields of view for three independent sets of experiments.

Neuroblastoma Cell Viability and Death Assays—Viable SH-SY5Y cells were quantified by using the CellTiter-Glo Luminescent Cell Viability Assay (Promega). Images were captured using the EVOS™ FL Cell Imaging System directly from culture plates under 10× magnification. Cell death was measured by the FITC Annexin V Apoptosis Detection Kit I (BD Biosciences) followed by LSR Fortessa II flow cytometry analysis. At least 10,000 cells were recorded per sample in each data set. In the cell death assay (Figure 3C), caspase inhibitor zVAD (Z-VAD-FMK; BD Biosciences) was added into the media upon α Syn induction (100 μ M final concentration). For the cell survival assay (Figure 3E), MPP+ iodide (1-methyl-4-phenylpyridinium iodide; Sigma) was added into media of transfected cells 48 hours before processing for cell viability assay.

Quantification and Statistical Analysis

Potential Target Site Analysis—Potential target sites for gRNAs 6-3 and 9-1 in the *S. cerevisiae* genome were identified using CasOT CRISPR off-target search tool (Xiao et al., 2014). All potential target sites with up to two mismatches inside the seed region are presented in Table S1.

Scoring Strategy for α Syn-toxicity Suppression in Yeast Survival Assays—A defined scoring system, which quantified the numbers of total and full spots in the spotting assays with serial dilutions, was used to score yeast survival upon α Syn induction: cells expressing the empty vector (which showed the least survival upon α Syn induction; sick

colonies in the first spot) were scored as 1, and samples overexpressing gRNA 9-1 and *UBP3* (the positive control for α Syn-toxicity suppression) were scored as 6 (five full spots and healthy colonies in the sixth spot). Other samples were scored by visual inspection and comparing the spotting assay survival results with the two abovementioned reference points.

Score	Number of total spots	Number of full spots	Score reference
6	6	5	<i>UBP3</i> and gRNA 9-1
5	5	4	
4	4	3	
3	3	2	
2	2	1	
1	1	0	Vector
0	0	0	

Scoring Strategy for α Syn Aggregate Suppression in Fluorescence

Microscopy Assays—A defined scoring system, which distinguished the percentage of cell-containing α Syn-YFP foci, was used to score α Syn-aggregate suppression: cells expressing the empty vector were scored as 1 (91.7%), and the samples overexpressing gRNA 9-1 were scored as 10 (6.5%).

Score	% cells with α Syn aggregates	Score reference
10	0 – 10%	gRNA 9-1
9	10 – 20%	
8	20 – 30%	
7	30 – 40%	
6	40 – 50%	
5	50 – 60%	
4	60 – 70%	
3	70 – 80%	
2	80 – 90%	
1	90 – 100%	Vector

Synergy Quantification—The increased survival against α Syn toxicity by overexpression of *TXN*, *TIMM9*, and *TXN*+ *TIMM9* was normalized to the vector control (Figure 3D) or the *EGFP* control (Figure 4B). We considered co-expression of *TXN*+ *TIMM9* to be interacting synergistically if the observed combination effect was greater than the expected effect given by Highest Single Agent (Borisov et al., 2003), Linear Interaction Effect (Slinker, 1998), and Bliss Independence (Greco et al., 1995) models. Synergy was calculated based on data presented in Figure 4B and tested by three models respectively, as illustrated in Figure 4C.

Data and Software Availability

The accession number for the RNA-Seq data reported in this paper is GEO: GSE87547. The sequences of recombinant DNA reported in this study have been deposited at Mendeley database (<http://dx.doi.org/10.17632/wfskh3hjj5.1>).

Additional Resources

Detailed Protocols—The protocols describe the procedures to construct and screen randomized gRNA library.

Supplementary Material

Refer to Web version on PubMed Central for supplementary material.

Acknowledgments

The ITox2C yeast strain was a generous gift from Susan Lindquist (Whitehead Institute, Cambridge, MA). We thank Leonidas Stefanis (Biomedical Research Foundation Academy of Athens, Athens, Greece) for SH-SY5Y cell lines. This work was supported by The Ellison Medical Foundation and the National Institutes of Health (1P50GM098792).

References

- Benjamini Y, Yosef Hochberg. Controlling the false discovery rate: a practical and powerful approach to multiple testing. *Journal of the Royal Statistical Society. Series B (Methodological)*. 1995;289–300.
- Blancafort P, Chen EI, Gonzalez B, Bergquist S, Zijlstra A, Guthy D, Brachat A, Brakenhoff RH, Quigley JP, Erdmann D, et al. Genetic reprogramming of tumor cells by zinc finger transcription factors. *Proc Natl Acad Sci U S A*. 2005; 102:11716–11721. [PubMed: 16081541]
- Bonifati V, Rizzu P, van Baren MJ, Schaap O, Breedveld GJ, Krieger E, Dekker MC, Squitieri F, Ibanez P, Joosse M, et al. Mutations in the DJ-1 gene associated with autosomal recessive early-onset parkinsonism. *Science*. 2003; 299:256–259. [PubMed: 12446870]
- Borisy AA, Elliott PJ, Hurst NW, Lee MS, Lehar J, Price ER, Serbedzija G, Zimmermann GR, Foley MA, Stockwell BR, et al. Systematic discovery of multicomponent therapeutics. *Proc Natl Acad Sci U S A*. 2003; 100:7977–7982. [PubMed: 12799470]
- Boutros M, Ahringer J. The art and design of genetic screens: RNA interference. *Nature reviews. Genetics*. 2008; 9:554–566.
- Canet-Aviles RM, Wilson MA, Miller DW, Ahmad R, McLendon C, Bandyopadhyay S, Baptista MJ, Ringe D, Petsko GA, Cookson MR. The Parkinson's disease protein DJ-1 is neuroprotective due to cysteine-sulfinic acid-driven mitochondrial localization. *Proc Natl Acad Sci U S A*. 2004; 101:9103–9108. [PubMed: 15181200]
- Carpenter AE, Sabatini DM. Systematic genome-wide screens of gene function. *Nature reviews. Genetics*. 2004; 5:11–22.
- Carroll D. Genome engineering with targetable nucleases. *Annual review of biochemistry*. 2014; 83:409–439.
- Cencic R, Miura H, Malina A, Robert F, Ethier S, Schmeing TM, Dostie J, Pelletier J. Protospacer adjacent motif (PAM)-distal sequences engage CRISPR Cas9 DNA target cleavage. *PLoS One*. 2014; 9:e109213. [PubMed: 25275497]
- Chandran J, Ding J, Cai H. Alsin and the molecular pathways of amyotrophic lateral sclerosis. *Molecular neurobiology*. 2007; 36:224–231. [PubMed: 17955197]
- Chavez A, Scheiman J, Vora S, Pruitt BW, Tuttle M, E PRI, Lin S, Kiani S, Guzman CD, Wiegand DJ, et al. Highly efficient Cas9-mediated transcriptional programming. *Nat Methods*. 2015; 12:326–328. [PubMed: 25730490]

- Chen YC, Kenworthy J, Gabrielse C, Hanni C, Zegerman P, Weinreich M. DNA replication checkpoint signaling depends on a Rad53-Dbf4 N-terminal interaction in *Saccharomyces cerevisiae*. *Genetics*. 2013; 194:389–401. [PubMed: 23564203]
- Chen YC, Weinreich M. Dbf4 regulates the Cdc5 Polo-like kinase through a distinct non-canonical binding interaction. *J Biol Chem*. 2010; 285:41244–41254. [PubMed: 21036905]
- Chung CY, Khurana V, Auluck PK, Tardiff DF, Mazzulli JR, Soldner F, Baru V, Lou Y, Freyzon Y, Cho S, et al. Identification and rescue of alpha-synuclein toxicity in Parkinson patient-derived neurons. *Science*. 2013; 342:983–987. [PubMed: 24158904]
- Cooper AA, Gitler AD, Cashikar A, Haynes CM, Hill KJ, Bhullar B, Liu K, Xu K, Strathearn KE, Liu F, et al. Alpha-synuclein blocks ER-Golgi traffic and Rab1 rescues neuron loss in Parkinson's models. *Science*. 2006; 313:324–328. [PubMed: 16794039]
- Costanzo M, VanderSluis B, Koch EN, Baryshnikova A, Pons C, Tan G, Wang W, Usaj M, Hanchard J, Lee SD, et al. A global genetic interaction network maps a wiring diagram of cellular function. *Science*. 2016; 353
- Demir K, Boutros M. Cell perturbation screens for target identification by RNAi. *Methods Mol Biol*. 2012; 910:1–13. [PubMed: 22821589]
- Dietz GP, Stockhausen KV, Dietz B, Falkenburger BH, Valbuena P, Opazo F, Lingor P, Meuer K, Weishaupt JH, Schulz JB, et al. Membrane-permeable Bcl-xL prevents MPTP-induced dopaminergic neuronal loss in the substantia nigra. *Journal of neurochemistry*. 2008; 104:757–765. [PubMed: 17995935]
- Durigon R, Wang Q, Ceh Pavia E, Grant CM, Lu H. Cytosolic thioredoxin system facilitates the import of mitochondrial small Tim proteins. *EMBO reports*. 2012; 13:916–922. [PubMed: 22878414]
- Escusa S, Laporte D, Massoni A, Boucherie H, Dautant A, Daignan-Fornier B. Skp1-Cullin-F-box-dependent degradation of Aah1p requires its interaction with the F-box protein Saf1p. *J Biol Chem*. 2007; 282:20097–20103. [PubMed: 17517885]
- Farzadfard F, Perli SD, Lu TK. Tunable and Multifunctional Eukaryotic Transcription Factors Based on CRISPR/Cas. *ACS Synth Biol*. 2013
- Forsburg SL. The art and design of genetic screens: yeast. *Nature reviews. Genetics*. 2001; 2:659–668.
- Frock RL, Hu J, Meyers RM, Ho YJ, Kii E, Alt FW. Genome-wide detection of DNA double-stranded breaks induced by engineered nucleases. *Nat Biotechnol*. 2015; 33:179–186. [PubMed: 25503383]
- Gilbert LA, Horlbeck MA, Adamson B, Villalta JE, Chen Y, Whitehead EH, Guimaraes C, Panning B, Ploegh HL, Bassik MC, et al. Genome-Scale CRISPR-Mediated Control of Gene Repression and Activation. *Cell*. 2014; 159:647–661. [PubMed: 25307932]
- Gilbert LA, Larson MH, Morsut L, Liu Z, Brar GA, Torres SE, Stern-Ginossar N, Brandman O, Whitehead EH, Doudna JA, et al. CRISPR-mediated modular RNA-guided regulation of transcription in eukaryotes. *Cell*. 2013; 154:442–451. [PubMed: 23849981]
- Gillis J, Schipper-Krom S, Juenemann K, Gruber A, Coolen S, van den Nieuwendijk R, van Veen H, Overkleeft H, Goedhart J, Kampinga HH, et al. The DNAJB6 and DNAJB8 protein chaperones prevent intracellular aggregation of polyglutamine peptides. *J Biol Chem*. 2013; 288:17225–17237. [PubMed: 23612975]
- Gitler AD, Chesi A, Geddie ML, Strathearn KE, Hamamichi S, Hill KJ, Caldwell KA, Caldwell GA, Cooper AA, Rochet JC, et al. Alpha-synuclein is part of a diverse and highly conserved interaction network that includes PARK9 and manganese toxicity. *Nature genetics*. 2009; 41:308–315. [PubMed: 19182805]
- Goedert M, Spillantini MG, Del Tredici K, Braak H. 100 years of Lewy pathology. *Nature reviews. Neurology*. 2013; 9:13–24. [PubMed: 23183883]
- Gouarne C, Tracz J, Paoli MG, Deluca V, Seimandi M, Tardif G, Xilouri M, Stefanis L, Bordet T, Pruss RM. Protective role of olesoxime against wild-type alpha-synuclein-induced toxicity in human neuronally differentiated SHSY-5Y cells. *British journal of pharmacology*. 2015; 172:235–245. [PubMed: 25220617]
- Greco WR, Bravo G, Parsons JC. The search for synergy: a critical review from a response surface perspective. *Pharmacological reviews*. 1995; 47:331–385. [PubMed: 7568331]

- Hadano S, Kunita R, Otomo A, Suzuki-Utsunomiya K, Ikeda JE. Molecular and cellular function of ALS2/alsin: implication of membrane dynamics in neuronal development and degeneration. *Neurochemistry international*. 2007; 51:74–84. [PubMed: 17566607]
- Han K, Jeng EE, Hess GT, Morgens DW, Li A, Bassik MC. Synergistic drug combinations for cancer identified in a CRISPR screen for pairwise genetic interactions. *Nat Biotechnol*. 2017; 35:463–474. [PubMed: 28319085]
- Henchcliffe C, Beal MF. Mitochondrial biology and oxidative stress in Parkinson disease pathogenesis. *Nature clinical practice. Neurology*. 2008; 4:600–609.
- Hilton IB, D'Ippolito AM, Vockley CM, Thakore PI, Crawford GE, Reddy TE, Gersbach CA. Epigenome editing by a CRISPR-Cas9-based acetyltransferase activates genes from promoters and enhancers. *Nat Biotechnol*. 2015; 33:510–517. [PubMed: 25849900]
- Horlbeck MA, Gilbert LA, Villalta JE, Adamson B, Pak RA, Chen Y, Fields AP, Park CY, Corn JE, Kampmann M, et al. Compact and highly active next-generation libraries for CRISPR-mediated gene repression and activation. *eLife*. 2016; 5
- Kearns NA, Pham H, Tabak B, Genga RM, Silverstein NJ, Garber M, Maehr R. Functional annotation of native enhancers with a Cas9-histone demethylase fusion. *Nat Methods*. 2015; 12:401–403. [PubMed: 25775043]
- Khurana V, Lindquist S. Modelling neurodegeneration in *Saccharomyces cerevisiae*: why cook with baker's yeast? *Nature reviews. Neuroscience*. 2010; 11:436–449. [PubMed: 20424620]
- Khurana V, Peng J, Chung CY, Auluck PK, Fanning S, Tardiff DF, Bartels T, Koeva M, Eichhorn SW, Benyamini H, et al. Genome-Scale Networks Link Neurodegenerative Disease Genes to alpha-Synuclein through Specific Molecular Pathways. *Cell systems*. 2017; 4:157–170. e114. [PubMed: 28131822]
- Konermann S, Brigham MD, Trevino AE, Joung J, Abudayyeh OO, Barcena C, Hsu PD, Habib N, Gootenberg JS, Nishimasu H, et al. Genome-scale transcriptional activation by an engineered CRISPR-Cas9 complex. *Nature*. 2015; 517:583–588. [PubMed: 25494202]
- Kosicek M, Wunderlich P, Walter J, Hecimovic S. GGA1 overexpression attenuates amyloidogenic processing of the amyloid precursor protein in Niemann-Pick type C cells. *Biochemical and biophysical research communications*. 2014; 450:160–165. [PubMed: 24866237]
- Kuscu C, Arslan S, Singh R, Thorpe J, Adli M. Genome-wide analysis reveals characteristics of off-target sites bound by the Cas9 endonuclease. *Nat Biotechnol*. 2014; 32:677–683. [PubMed: 24837660]
- Lashuel HA, Overk CR, Oueslati A, Masliah E. The many faces of alpha-synuclein: from structure and toxicity to therapeutic target. *Nature reviews. Neuroscience*. 2013; 14:38–48. [PubMed: 23254192]
- Lin MT, Beal MF. Mitochondrial dysfunction and oxidative stress in neurodegenerative diseases. *Nature*. 2006; 443:787–795. [PubMed: 17051205]
- Lois C, Hong EJ, Pease S, Brown EJ, Baltimore D. Germline transmission and tissue-specific expression of transgenes delivered by lentiviral vectors. *Science*. 2002; 295:868–872. [PubMed: 11786607]
- MacQuarrie KL, Fong AP, Morse RH, Tapscott SJ. Genome-wide transcription factor binding: beyond direct target regulation. *Trends in genetics : TIG*. 2011; 27:141–148. [PubMed: 21295369]
- Mali P, Aach J, Stranges PB, Esvelt KM, Moosburner M, Kosuri S, Yang L, Church GM. CAS9 transcriptional activators for target specificity screening and paired nickases for cooperative genome engineering. *Nat Biotechnol*. 2013; 31:833–838. [PubMed: 23907171]
- Maries E, Dass B, Collier TJ, Kordower JH, Steece-Collier K. The role of alpha-synuclein in Parkinson's disease: insights from animal models. *Nature reviews. Neuroscience*. 2003; 4:727–738. [PubMed: 12951565]
- Mark KG, Simonetta M, Maiolica A, Seller CA, Toczyski DP. Ubiquitin ligase trapping identifies an SCF(Saf1) pathway targeting unprocessed vacuolar/lysosomal proteins. *Mol Cell*. 2014; 53:148–161. [PubMed: 24389104]
- Moffat J, Grueneberg DA, Yang X, Kim SY, Kloepfer AM, Hinkle G, Piqani B, Eisenhaure TM, Luo B, Grenier JK, et al. A lentiviral RNAi library for human and mouse genes applied to an arrayed viral high-content screen. *Cell*. 2006; 124:1283–1298. [PubMed: 16564017]

- Neupert W, Herrmann JM. Translocation of proteins into mitochondria. Annual review of biochemistry. 2007; 76:723–749.
- Nishimasu H, Ran FA, Hsu PD, Konermann S, Shehata SI, Dohmae N, Ishitani R, Zhang F, Nureki O. Crystal structure of Cas9 in complex with guide RNA and target DNA. Cell. 2014; 156:935–949. [PubMed: 24529477]
- O'Geen H, Henry IM, Bhakta MS, Meckler JF, Segal DJ. A genome-wide analysis of Cas9 binding specificity using ChIP-seq and targeted sequence capture. Nucleic acids research. 2015; 43:3389–3404. [PubMed: 25712100]
- Outeiro TF, Lindquist S. Yeast cells provide insight into alpha-synuclein biology and pathobiology. Science. 2003; 302:1772–1775. [PubMed: 14657500]
- Park KS, Lee DK, Lee H, Lee Y, Jang YS, Kim YH, Yang HY, Lee SI, Seol W, Kim JS. Phenotypic alteration of eukaryotic cells using randomized libraries of artificial transcription factors. Nat Biotechnol. 2003; 21:1208–1214. [PubMed: 12960965]
- Parnas O, Jovanovic M, Eisenhaure TM, Herbst RH, Dixit A, Ye CJ, Przybylski D, Platt RJ, Tirosch I, Sanjana NE, et al. A Genome-wide CRISPR Screen in Primary Immune Cells to Dissect Regulatory Networks. Cell. 2015; 162:675–686. [PubMed: 26189680]
- Paulsen RD, Soni DV, Wollman R, Hahn AT, Yee MC, Guan A, Hesley JA, Miller SC, Cromwell EF, Solow-Cordero DE, et al. A genome-wide siRNA screen reveals diverse cellular processes and pathways that mediate genome stability. Mol Cell. 2009; 35:228–239. [PubMed: 19647519]
- Robinson MD, Grigull J, Mohammad N, Hughes TR. FunSpec: a web-based cluster interpreter for yeast. BMC bioinformatics. 2002; 3:35. [PubMed: 12431279]
- Root DE, Hacohen N, Hahn WC, Lander ES, Sabatini DM. Genome-scale loss-of-function screening with a lentiviral RNAi library. Nat Methods. 2006; 3:715–719. [PubMed: 16929317]
- Santos CN, Stephanopoulos G. Combinatorial engineering of microbes for optimizing cellular phenotype. Curr Opin Chem Biol. 2008; 12:168–176. [PubMed: 18275860]
- Shalem O, Sanjana NE, Hartenian E, Shi X, Scott DA, Mikkelsen TS, Heckl D, Ebert BL, Root DE, Doench JG, et al. Genome-scale CRISPR-Cas9 knockout screening in human cells. Science. 2014; 343:84–87. [PubMed: 24336571]
- Shen JP, Zhao D, Sasik R, Luebeck J, Birmingham A, Bojorquez-Gomez A, Licon K, Klepper K, Pekin D, Beckett AN, et al. Combinatorial CRISPR-Cas9 screens for de novo mapping of genetic interactions. Nat Methods. 2017
- Slinker BK. The statistics of synergism. Journal of molecular and cellular cardiology. 1998; 30:723–731. [PubMed: 9602421]
- Spillantini MG, Schmidt ML, Lee VM, Trojanowski JQ, Jakes R, Goedert M. Alpha-synuclein in Lewy bodies. Nature. 1997; 388:839–840. [PubMed: 9278044]
- Takatsu H, Yoshino K, Toda K, Nakayama K. GGA proteins associate with Golgi membranes through interaction between their GGAH domains and ADP-ribosylation factors. The Biochemical journal. 2002; 365:369–378. [PubMed: 11950392]
- Tanenbaum ME, Gilbert LA, Qi LS, Weissman JS, Vale RD. A protein-tagging system for signal amplification in gene expression and fluorescence imaging. Cell. 2014; 159:635–646. [PubMed: 25307933]
- Tardiff DF, Jui NT, Khurana V, Tambe MA, Thompson ML, Chung CY, Kamadurai HB, Kim HT, Lancaster AK, Caldwell KA, et al. Yeast reveal a "druggable" Rsp5/Nedd4 network that ameliorates alpha-synuclein toxicity in neurons. Science. 2013; 342:979–983. [PubMed: 24158909]
- Tardiff DF, Khurana V, Chung CY, Lindquist S. From yeast to patient neurons and back again: powerful new discovery platform. Movement disorders : official journal of the Movement Disorder Society. 2014; 29:1231–1240. [PubMed: 25131316]
- Tenreiro S, Rosado-Ramos R, Gerhardt E, Favretto F, Magalhaes F, Popova B, Becker S, Zweckstetter M, Braus GH, Outeiro TF. Yeast reveals similar molecular mechanisms underlying alpha- and beta-synuclein toxicity. Hum Mol Genet. 2016; 25:275–290. [PubMed: 26586132]
- Thakore PI, D'Ippolito AM, Song L, Safi A, Shivakumar NK, Kabadi AM, Reddy TE, Crawford GE, Gersbach CA. Highly specific epigenome editing by CRISPR-Cas9 repressors for silencing of distal regulatory elements. Nat Methods. 2015; 12:1143–1149. [PubMed: 26501517]

- Tsai CJ, Aslam K, Drendel HM, Asiago JM, Goode KM, Paul LN, Rochet JC, Hazbun TR. Hsp31 Is a Stress Response Chaperone That Intervenes in the Protein Misfolding Process. *J Biol Chem.* 2015; 290:24816–24834. [PubMed: 26306045]
- Vekrellis K, Xilouri M, Emmanouilidou E, Stefanis L. Inducible over-expression of wild type alpha-synuclein in human neuronal cells leads to caspase-dependent non-apoptotic death. *Journal of neurochemistry.* 2009; 109:1348–1362. [PubMed: 19476547]
- von Einem B, Wahler A, Schips T, Serrano-Pozo A, Proepper C, Boeckers TM, Rueck A, Wirth T, Hyman BT, Danzer KM, et al. The Golgi-Localized gamma-Ear-Containing ARF-Binding (GGA) Proteins Alter Amyloid-beta Precursor Protein (APP) Processing through Interaction of Their GAE Domain with the Beta-Site APP Cleaving Enzyme 1 (BACE1). *PLoS One.* 2015; 10:e0129047. [PubMed: 26053850]
- Vos MJ, Hageman J, Carra S, Kampinga HH. Structural and functional diversities between members of the human HSPB, HSPH, HSPA, and DNAJ chaperone families. *Biochemistry.* 2008; 47:7001–7011. [PubMed: 18557634]
- Wang T, Wei JJ, Sabatini DM, Lander ES. Genetic screens in human cells using the CRISPR-Cas9 system. *Science.* 2014; 343:80–84. [PubMed: 24336569]
- Whitehurst AW, Bodemann BO, Cardenas J, Ferguson D, Girard L, Peyton M, Minna JD, Michnoff C, Hao W, Roth MG, et al. Synthetic lethal screen identification of chemosensitizer loci in cancer cells. *Nature.* 2007; 446:815–819. [PubMed: 17429401]
- Wong AS, Choi GC, Cheng AA, Purcell O, Lu TK. Massively parallel high-order combinatorial genetics in human cells. *Nat Biotechnol.* 2015; 33:952–961. [PubMed: 26280411]
- Wong AS, Choi GC, Cui CH, Pregernig G, Milani P, Adam M, Perli SD, Kazer SW, Gaillard A, Hermann M, et al. Multiplexed barcoded CRISPR-Cas9 screening enabled by CombiGEM. *Proc Natl Acad Sci U S A.* 2016; 113:2544–2549. [PubMed: 26864203]
- Wong YC, Krainc D. alpha-synuclein toxicity in neurodegeneration: mechanism and therapeutic strategies. *Nature medicine.* 2017; 23:1–13.
- Wu X, Scott DA, Kriz AJ, Chiu AC, Hsu PD, Dadon DB, Cheng AW, Trevino AE, Konermann S, Chen S, et al. Genome-wide binding of the CRISPR endonuclease Cas9 in mammalian cells. *Nat Biotechnol.* 2014; 32:670–676. [PubMed: 24752079]
- Xiao A, Cheng Z, Kong L, Zhu Z, Lin S, Gao G, Zhang B. CasOT: a genome-wide Cas9/gRNA off-target searching tool. *Bioinformatics.* 2014
- Yeger-Lotem E, Riva L, Su LJ, Gitler AD, Cashikar AG, King OD, Auluck PK, Geddie ML, Valastyan JS, Karger DR, et al. Bridging high-throughput genetic and transcriptional data reveals cellular responses to alpha-synuclein toxicity. *Nature genetics.* 2009; 41:316–323. [PubMed: 19234470]
- Zalatan JG, Lee ME, Almeida R, Gilbert LA, Whitehead EH, La Russa M, Tsai JC, Weissman JS, Dueber JE, Qi LS, et al. Engineering complex synthetic transcriptional programs with CRISPR RNA scaffolds. *Cell.* 2015; 160:339–350. [PubMed: 25533786]
- Zhang F, Cong L, Lodato S, Kosuri S, Church GM, Arlotta P. Efficient construction of sequence-specific TAL effectors for modulating mammalian transcription. *Nat Biotechnol.* 2011; 29:149–153. [PubMed: 21248753]
- Zhdankina O, Strand NL, Redmond JM, Boman AL. Yeast GGA proteins interact with GTP-bound Arf and facilitate transport through the Golgi. *Yeast (Chichester, England).* 2001; 18:1–18.
- Zondler L, Miller-Fleming L, Repici M, Goncalves S, Tenreiro S, Rosado-Ramos R, Betzer C, Straatman KR, Jensen PH, Giorgini F, et al. DJ-1 interactions with alpha-synuclein attenuate aggregation and cellular toxicity in models of Parkinson's disease. *Cell Death Dis.* 2014; 5:e1350. [PubMed: 25058424]

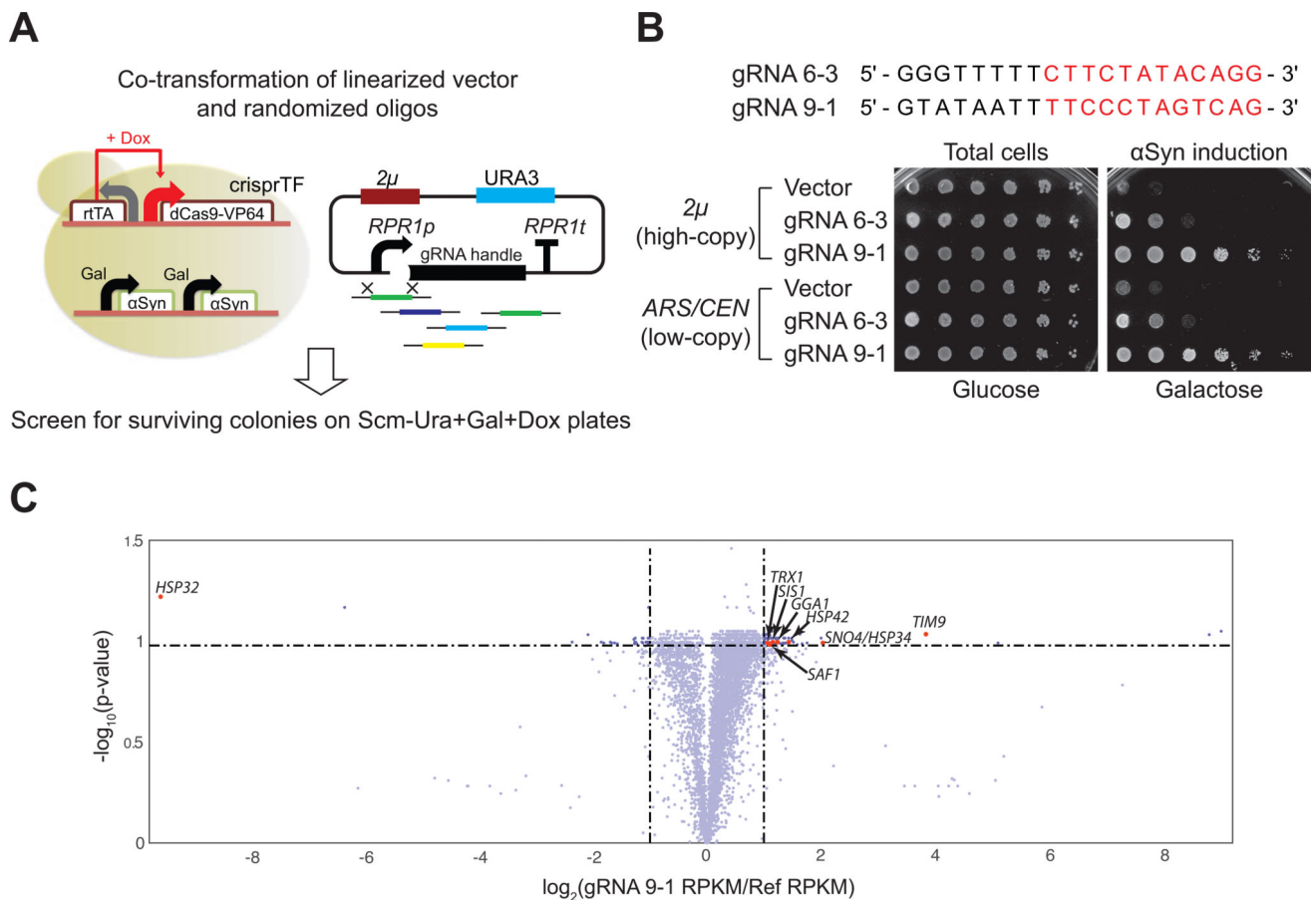


Figure 1. Randomized gRNA/crisprTF screens identify genetic modifiers of αSyn toxicity in *S. cerevisiae*

(A) Schematic illustration of the engineered yeast screen strain expressing αSyn and crisprTF (left) and the strategy used for building the randomized gRNA library (right). See Methods section and Figures S1–S2 for details. (B) Sequences of the two identified gRNAs (designated as gRNA 6-3 and 9-1) that could suppress αSyn-mediated toxicity. 5-fold serial dilutions of saturated cultures were spotted on Scm (Synthetic complete media)–Uracil (Ura)+Glucose+Doxycycline (Dox) plates to quantify the total number of viable cells and Scm–Ura+Galactose (Gal)+Dox plates to score cell viability upon αSyn induction. gRNA 9-1 is a strong suppressor of αSyn toxicity while gRNA 6-3 is a moderate suppressor. Both gRNAs performed better than the negative control (empty vector), and suppression levels were independent of gRNA plasmid copy number. See also Figure S1. (C) The transcriptome analysis of the screen strain harboring gRNA 9-1 in comparison with the reference strain (screen strain with no gRNA) represented as a volcano plot (x-axis: fold change versus y-axis: statistical significance). A list of differentially expressed genes is provided in Table S2.

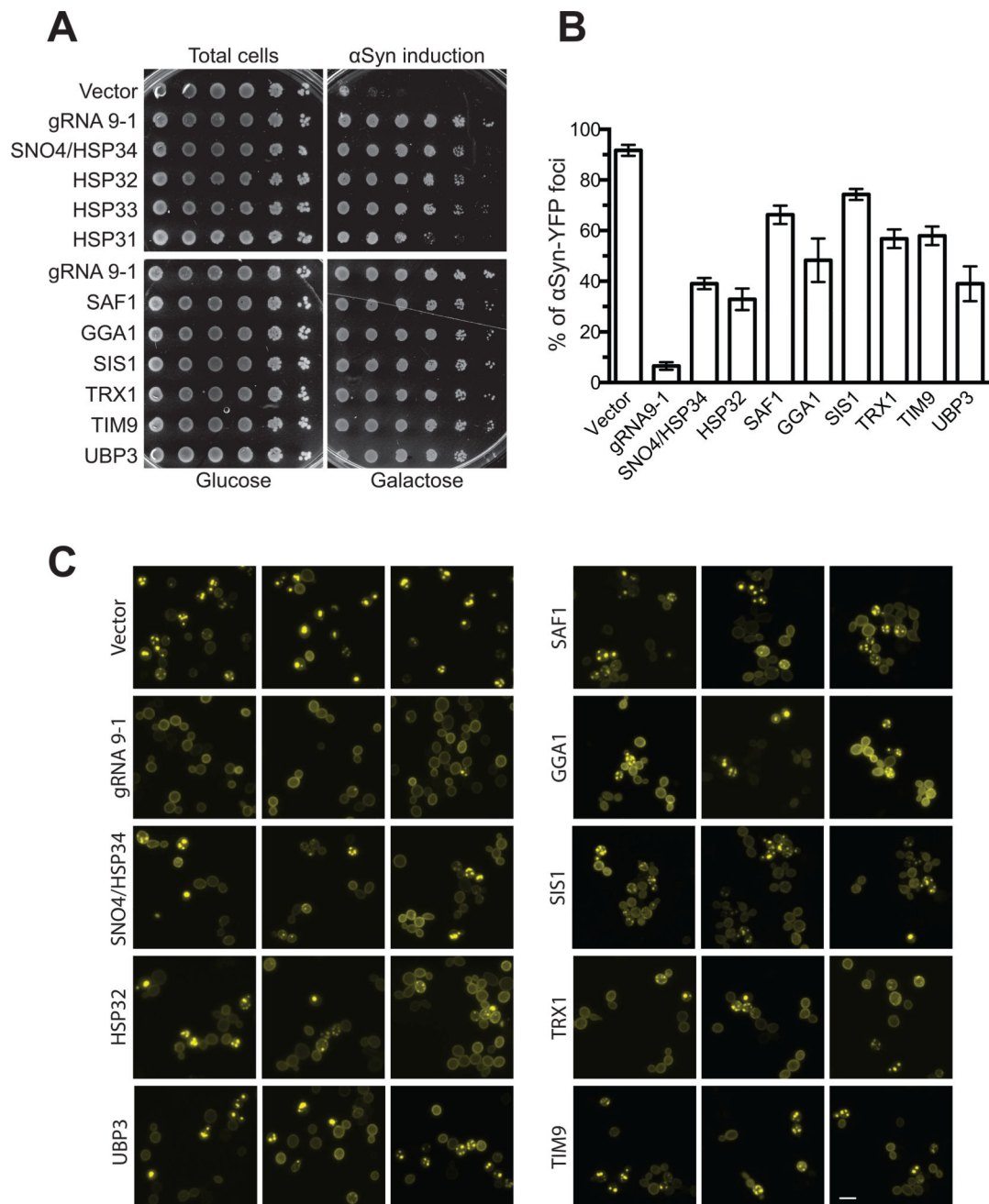


Figure 2. Overexpressing genes identified from the gRNA 9-1/crisprTF screen rescues α Syn-associated cellular defects in yeast

(A) Survival of the screen strain harboring gRNA 9-1 ('gRNA 9-1') compared to cells expressing the empty vector ('Vector') and those overexpressing *HSP31–34* (heat shock proteins) (top) as well as top-ranked α Syn suppressors identified in the screen (bottom). *UBP3*, a known strong α Syn suppressor, was used as a positive control. (B) Quantification of α Syn-YFP foci in the screen strain harboring either no gRNA or gRNA 9-1, or cells harboring plasmids that overexpress the indicated genes. Cytoplasmic YFP foci represent α Syn aggregates produced as a result of defects in vesicular trafficking. Cells expressing crisprTF and gRNA 9-1 robustly inhibited α Syn aggregates, evidenced by the absence of

cytoplasmic YFP foci in these samples. Cells overexpressing *UBP3* were used as a positive control in this assay. Data were presented as mean \pm SEM of three biological replicates. (C) Representative images of α Syn-expressing cells mentioned in **b**. Bar = 10 μ m. See also Figures S3–S4.

Author Manuscript

Author Manuscript

Author Manuscript

Author Manuscript

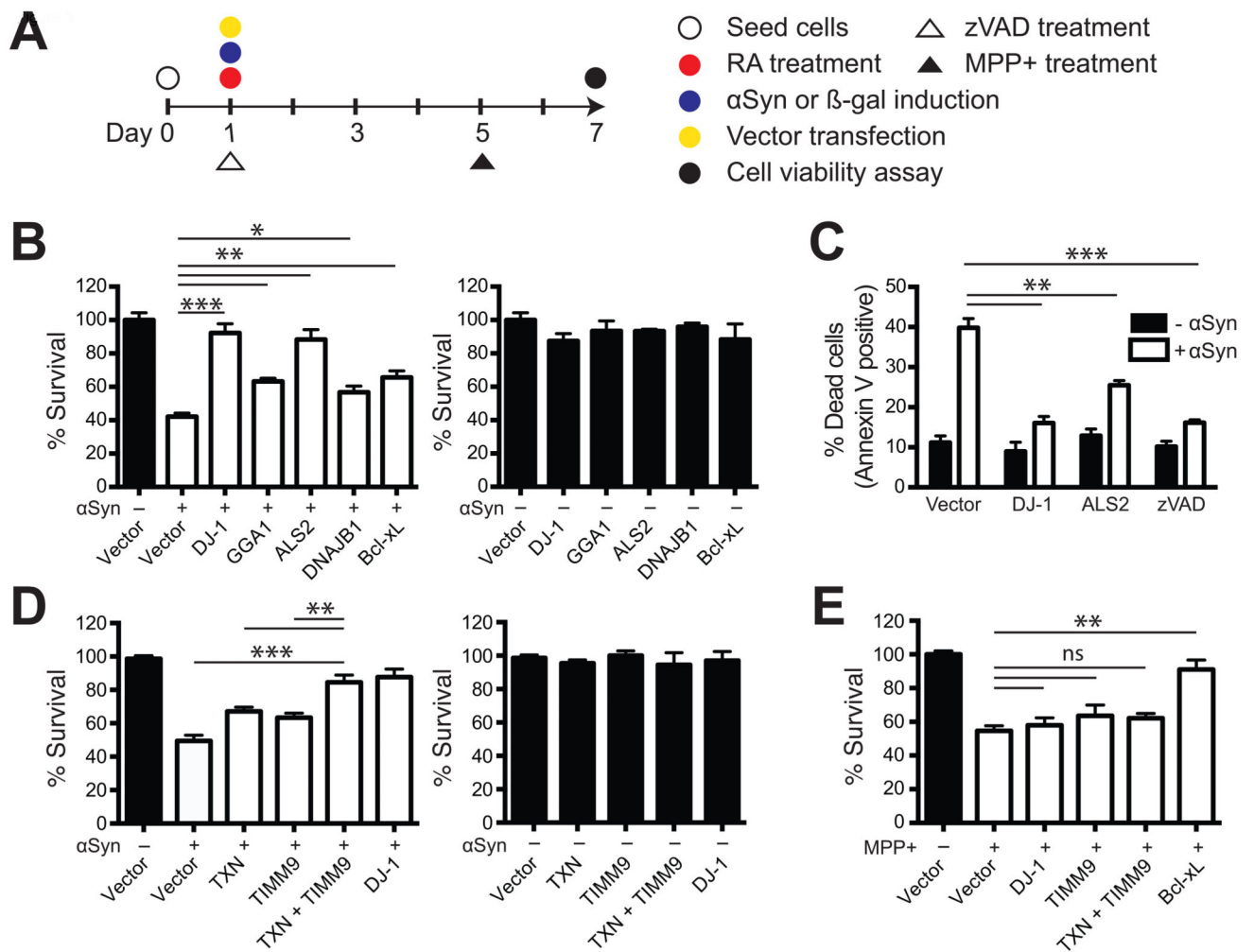


Figure 3. Human homologs of yeast α Syn-toxicity suppressors in a human neuronal PD model

(A) A schematic representation of the experimental procedure used to test the human homologs of yeast α Syn-toxicity suppressors in differentiated neuronal cell lines. Different constructs expressing individual genes were transfected into the SH-SY5Y neuroblastoma cell line via transient transfection to examine their ability to protect against α Syn toxicity. α Syn expression was induced by removal of Dox from the media and retinoic acid (RA) treatment was used for neuronal differentiation over the course of a six-day period. The anti-cell-death drug zVAD and the toxin MPP⁺ were applied in control experiments. See also Figure S5. (B) Cell viability of differentiated cell lines overexpressing α Syn and the indicated constructs (white bars) were determined by the CellTiter-Glo luminescent assay. The expression of individual genes did not significantly affect cell survival of differentiated cells in the absence of α Syn induction (black bars). Constructs expressing human *DJ-1* (homolog of yeast *SNO4/HSP34* and *HSP32*), *GGA1* (*GGA1*), *ALS2* (*SAF1*), or *DNAJB1* (*SIS1*) were tested. *Bcl-xL*, which protects against apoptotic neuronal death, was used a positive control (Dietz et al., 2008). (C) The percentage of dead cells upon α Syn induction was quantitated by FITC-Annexin V staining followed by flow cytometry. Effects of overexpressing *DJ-1* or *ALS2* via plasmid transfection were compared with effects of zVAD.

(D) Constructs expressing human *TXN* (homolog of yeast *TRX1*) or *TIMM9* (homolog of yeast *TIM9*) were transfected individually or co-transfected together to test for synergistic effects on protection from α Syn toxicity. *TXN* + *TIMM9* synergistically rescued these cells from α Syn toxicity when co-transfected together. **(E)** Overexpression of *DJ-1*, *TIMM9*, or *TXN* + *TIMM9* did not protect against MPP+ toxicity, in contrast with *Bcl-xL* overexpression. Transfected and differentiated cells were treated with 6 mM MPP+ and then tested for cell viability 48 hours afterwards. All data were presented as mean \pm SEM of triplicate sets. * $p < 0.05$, ** $p < 0.01$, *** $p < 0.001$; ns, not significant.

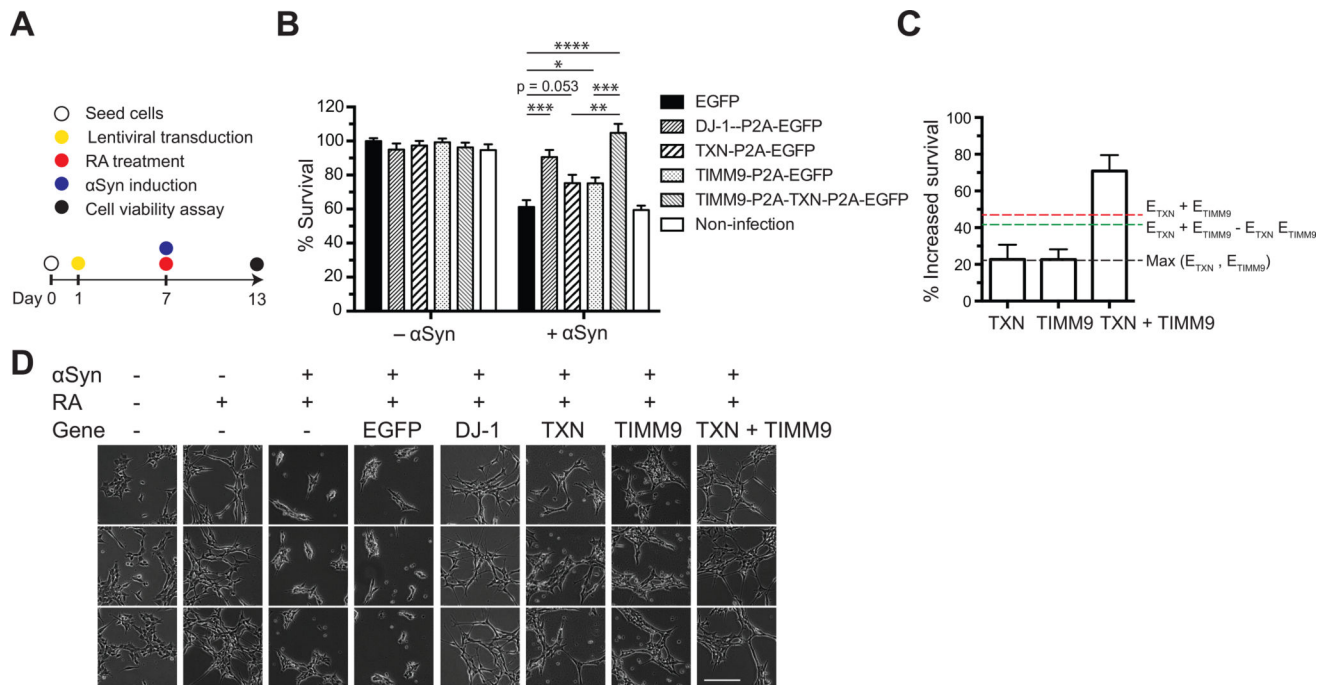


Figure 4. Lentiviral expression of human *DJ-1*, *TXN*, and *TIMM9* protects against αSyn-associated toxicity in a neuronal PD model

(A) The human homologs of yeast αSyn-toxicity suppressors were stably expressed via lentiviral vectors six days before RA treatment and αSyn induction, as indicated in the experimental procedure diagram. (B) Overexpression of *DJ-1* or *TXN* + *TIMM9* significantly increased neuronal viability in the presence of αSyn. The 2A peptide sequence (P2A) was used to achieve the simultaneous expression of multiple genes from a single promoter. (C) *TXN* and *TIMM9* work synergistically protect neuronal cells from αSyn toxicity based on Highest Single Agent [$\text{Max}(E_{TXN}, E_{TIMM9})$] (Borisy et al., 2003), Linear Interaction Effect ($E_{TXN} + E_{TIMM9}$) (Slinker, 1998), and Bliss Independence ($E_{TXN} + E_{TIMM9} - E_{TXN} E_{TIMM9}$) (Greco et al., 1995) models (dashed lines). The effect of *TXN* + *TIMM9* was greater than the threshold values obtained from these models. (D) Representative images of neuronal morphology and cell density of cells transfected with lentiviral vectors overexpressing the indicated human genes. Bar = 400 μm. All data were presented as mean ± SEM, n = 6. *p < 0.05, **p < 0.01, ***p < 0.001, ****p < 0.0001.

A summary of top-ranked genes that are differentially regulated by gRNA 9-1 and that suppressed α Syn toxicity in yeast when overexpressed. A complete list of genes differentially modulated by gRNA 9-1 is provided in Table S2.

Table 1

Yeast Gene	Human Homologs	Log ₂ (fold change)	Survival Score	Fluorescent Foci Score	Biological Function
<i>SNO4/HSP34</i>	<i>DI-1/PARK7</i>	2.035	6	7	Chaperone and cysteine protease
<i>HSP32</i>	<i>DI-1/PARK7</i>	-9.593	6	7	Chaperone and cysteine protease
<i>HSP42</i>	<i>HSPB1, HSPB3, HSPB6, HSPB7, HSPB8, HSPB9</i>	1.434	5	6	Chaperone
<i>SIS1</i>	<i>DNAJB1-B9</i>	1.154	6	3	Chaperone
<i>GGA1</i>	<i>GGA1, GGA2, GGA3</i>	1.241	6	6	ER to Golgi vesicular trafficking
<i>SRN2</i>		1.031	6	4	Ubiquitin-dependent protein sorting
<i>SAF1</i>	<i>ALS2, RCC1</i>	1.180	6	4	Proteasome-dependent degradation
<i>TRX1</i>	<i>TXN, TXNDC2, TXNDC8</i>	1.072	6	5	Thioredoxin
<i>TIM9</i>	<i>TIMM9</i>	3.846	6	5	Mitochondrial intermembrane protein
<i>OXR1</i>	<i>OXR1, NCOA7, TLDC2</i>	1.003	5	3	Oxidative damage resistance
<i>STF2</i>	<i>SERBP1, HABP4</i>	2.004	6	3	mRNA stabilization
gRNA 9-1			6	10	
<i>UBP3</i>			6	7	
Vector			1	1	